Evaluation of a Friction Reduction Based Haptic Surface at High Frequency

Frédéric Giraud, Tomohiro Hara, Christophe Giraud-Audine, Michel Amberg, Betty Lemaire-Semail, Masaya Takasaki

Evaluation of a Friction Reduction Based Haptic Surface at High Frequency

Frédéric Giraud[1], Tomohiro Hara[2], Christophe Giraud-Audine[1], Michel Amberg [1], Betty Lemaire-Semail[1], and Masaya Takasaki[2]

***Abstract*— The influence of the vibration frequency on the friction reduction of an ultrasonic haptic surface has been reported in the literature. The models predict that increasing the frequency of the vibration leads to higher friction reduction at constant vibration amplitude, but this has not been reported experimentally. In this paper, we study the friction reduction on a prototype which can vibrate at low (66kHz) and high (225kHz) frequency. By estimating the *Point of Subjective Equivalence* between a standard at low frequency with a sample at high frequency, we have found that high frequencies can indeed reduce the friction, with the advantage of much smaller vibration amplitude. Moreover, we show that the invariant between the two frequency conditions is not the vibration amplitude. Our conclusion is that the invariant could be the acceleration instead.**

I. INTRODUCTION

The haptic Surfaces can change how a user perceives them. For instance, they can create the sensation of roughness on a flat plate of copper [1], of texture on a LCD display [2], improve the recognition of 3d shapes on a touchscreen [3] or create localized tactile feedback [4]. The operating principle of these tactile displays is to modulate the forces between the user's fingertip and the surface. Indeed, lateral forces can encode the information of roughness and geometry, and researchers have found ways to dynamically change the friction forces when a user's fingertip slides on a surface. Electrovibration [5] or electroadhesion [6] use the electrostatic force produced when a high voltage gradient is created between the finger and the surface to increase the friction. Instead, in this paper we use ultrasonic vibrations of the plate at several tens of kilohertz to reduce the friction.

The design of haptic surfaces using ultrasonic vibrations have been widely studied. In [7], the design requirements are laid down, considering that a *squeeze film air bearing* is produced by the vibration. The study is further elaborated in [8] which uses a lumped parameters model to optimize the dimension of the device. These works however consider ultrasonic vibrations between 40kHz and 60kHz at vibration amplitude in the range of the micrometer. These devices could take benefit of higher frequencies, leading to smaller vibration wavelength, smaller actuators and also smaller vibration amplitude [9]. In [10] surface acoustic waves at 15MHz have been used with vibration in the range of the nanometer to create a friction reduction. However, because high frequency vibrations penetrates into the skin, a direct contact between the fingertip and the surface acoustic waves cannot be possible.

This paper investigates an intermediate frequency, higher than our existing prototypes yet allowing a direct contact with the vibrating plate. We have chosen $f = 200$kHz. For that purpose, the first section exploits a modelling of the friction reduction, so as to estimate the required vibration amplitude in order to reduce the friction below a threshold. Then, a prototype at 200kHz is designed in the second section, and tested through an experimental study.

II. BED SPRING MODEL OF THE FRICTION REDUCTION

A. Model's Background

When a user's fingertip touches a vibrating plate, the skin of the pulp bounces, and this phenomenon has been reported in the literature [9], [11]. This phenomenon alone doesn't explain the friction reduction. Therefore, additional theories have been used, it order to estimate the reduction of friction for a given vibration amplitude. The squeeze film effect theory [7] calculates the overpressure due to the non-linear compression of the air in the gap between the finger pulp and the surface while the reduction of the contact area can also explain the friction reduction. In [9], the active lubrication theory considers the fingertip as an elastic body, and takes into account the difference between the static and

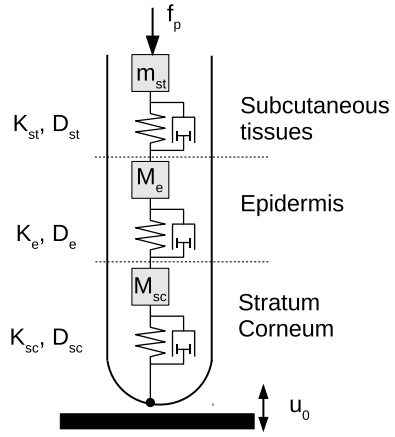

Fig. 1. Bed spring model of the finger pulp in the normal direction.

*This work has been carried out within the framework of the Mint project of IRCICA (Institut de de Recherche sur les Composants Logiciels et Matériel pour la communication avancée) and Inria.

[1]Frédéric Giraud, Michel Amberg, and Betty Lemaire-Semail are with Univ. Lille, Centrale Lille, Arts et Métiers Paris Tech, HEI, EA 2697 - L2EP -Laboratoire dElectrotechnique et dElectronique de Puissance, F-59000 Lille, France frederic.giraud@univ-lille1.fr

[2]Tomohiro Hara and Masaya Takasaki are with the Department of Mechanical Engineering, Saitama University, Shimo-Okubo 255, Sakura-ku, Saitama 338-8570, Japan

the dynamic friction coefficient. Since Vezzoli and al didn't investigate the model at frequency higher than 100kHz we explore the models result above 200kHz.

The model of the pulp is laid down for the normal and tangential axis. Along the normal axis, we consider in the figure 1 the pulp composed of 3 layers of elastic materials, representing respectively the stratum-corneum, the dermis and the subcutaneous tissues, and which are denoted by sc, d and st respectively. Each layer has its own stiffness, equivalent mass and damping, denoted by K_i, M_i and D_i with $i \in \{sc, d, st\}$. The input to this model is the pre-load force f_p of the user on the plate which is set on the subcutaneous tissues, and the vibration speed of the plate u_o. Depending on the position of the vibrating plate, we define two states for the model. In the state "contact", the pulp is touching the vibrating plate; during this state, the speed of the finger pulp equals that of the plate. In the state "flying", the pulp and the plate are not in contact, and the contact force f_{Nsc} is null.

On the tangential axis, we consider a stick-slip behaviour as explained figure 2 which derives from the Coulomb's theory of contact. The finger pulp is moving at constant speed v_F along the tangential direction. When the normal state is "flying", there is no contact force and the tangential force f_{Tsc} is equal to 0. When the contact occurs, the pulp first sticks on the plate; this is the "sticking" state on the tangential axis. When sticking, the pulp is stretching as one end is fixed, while the other is moving at constant speed, and we name x_T the pulp's deflection. Due to the finger's stiffness in the tangential direction, denoted by K_{Tsc}, f_{Tsc} increases. When f_{Tsc} reaches a limit value, equal to μf_{Nsc} where μ is named the friction coefficient, the pulp starts to slide: this is the "sliding" state, and the tangential force f_{Tsc} equals μf_{Nsc}. The flying state is detected when the contact force f_{Nsc} reaches 0. This behaviour can be represented by the state machine in the figure 2.

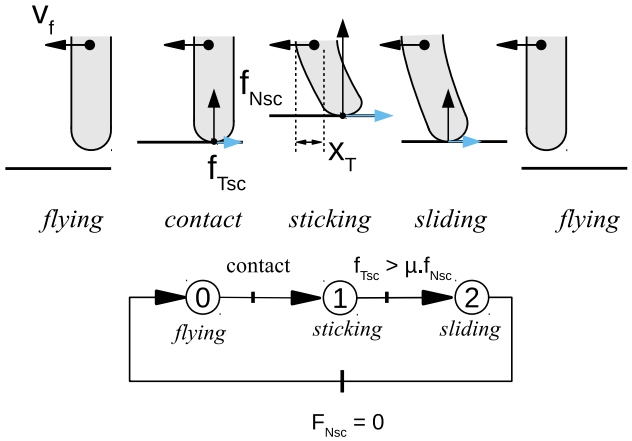

Fig. 2. Stick-slip on the tangential direction, and the corresponding state-machine.

B. Matlab Simulink Implementation

The model of the tangential and normal axis have been implemented into Matlab-Simulink (TM). In the normal axis, the mass-spring systems are simulated using first order transfer functions. For that purpose, we introduce the internal state variables of the speed of the mass M_i denoted by u_i and the force of the spring K_i denoted by f_{Ni} with $i \in \{sc, d, st\}$. The modelling of the figure 1 leads then to write:

$$f_{Nj} = K_j \int (u_i - u_j)\mathrm{d}t - D_j u_j \tag{1}$$

and

$$u_j = \frac{1}{M_j} \int (F_{Ni} - F_{Nk})\,\mathrm{d}t \tag{2}$$

with $\{i, j, k\} = \{o, sc, e\}$ or $\{sc, e, st\}$ or $\{e, st, b\}$, depending on which layer is considered. To take into account the two states (contact and flying), it is necessary that the force f_{Nsc} cannot be lower than 0. For that purpose, a saturated integrator from simulink is used, with a low saturation value set to 0. The saturation port's output is set to -1 when the integrator saturates, and can be used as a state indicator for the normal axis. The typical implementation for the mass-spring system of the stratum corneum is then given in the figure 3. On the tangential axis, the state-machine

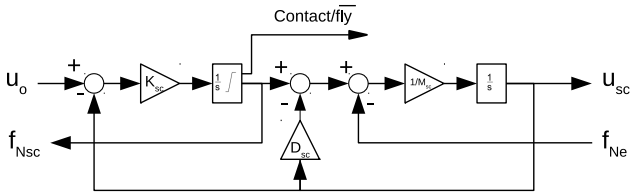

Fig. 3. Stick-slip on the tangential direction, and the corresponding state-machine.

in the figure 2 is directly implemented using the simulink toolbox "stateflow". The algorithms to calculate the two state variables X_T and f_{Tsc} depend on the state:

- flying and sliding: $X_T = 0$ and $f_{Tsc} = \mu f_{Nsc}$,
- sticking $X_T = \int V_F \mathrm{d}t$ and $f_{Tsc} = K_{Tsc} X_T$.

Therefore, the simulink implementation uses a selector, which output depends on the contact condition, as described in the figure 4.

C. Simulation results

The parameters used for the simulation are summarized table I. They were extracted from [9] for a normal force of $f_t = 0.5N$. This set of parameters are used because they were validated for a large frequency span. The damping values are tuned in order to achieve a critical damping of each layer. The simulations in Matlab are achieved with a variable step algorithm (ode113) with relative and absolute errors set to 10^-9. A maximum step size of 100ns is set, in order to locate the transitions of the stateflow variables.

We present in the figure 5 the simulation result of the forces f_{Nsc} and f_{Tsc} as a function of time, for a vibration amplitude of 100nm peak to peak, a finger speed V_F equal to

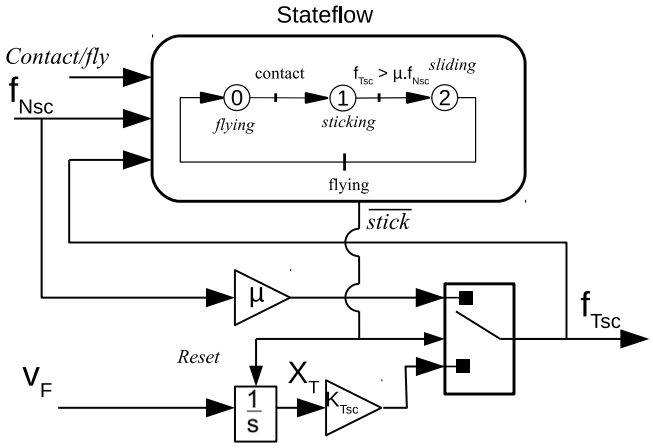

Fig. 4. Simulink implementation of the model in the tangential axis.

K_e	2170N.mm^{-1}
K_{sc}	8700 N.mm^{-1}
K_{sT}	1 N.mm^{-1}
M_e	0.04 g
M_{sc}	0.01 g
M_{sT}	0.12 g
K_{Tsc}	98120N.mm^{-1}

TABLE I

PARAMETERS USED FOR THE SIMULATION.

0.1m/s^{-1}, and a friction coefficient μ of 1. The normal force f_p applied onto the subcutaneous tissue is equal to 0.5N. In this figure, we have also depicted the three states of contact.

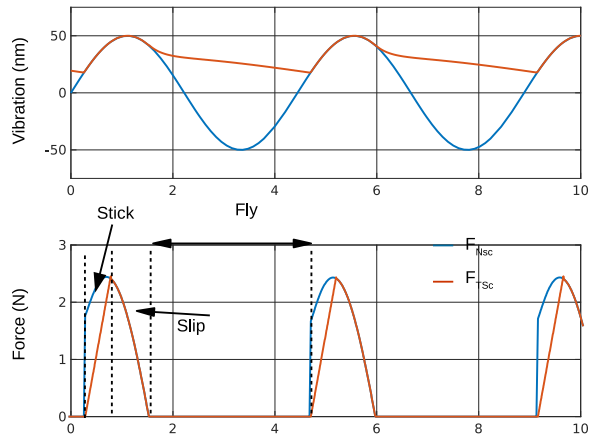

Fig. 5. Simulation results of the normal and tangential force.

By averaging the tangential force, it is possible to calculate the coefficient of friction μ_{US} with ultrasonic vibrations. By changing the vibration amplitude, it is possible to draw the evolution of the friction coefficient as a function of the vibration amplitude, for a low (66kHz) and a high (225kHz) frequency, as presented in the figure 6.

Hence, by extending the result to the high frequencies, the model predicts that there is a friction reduction at 225kHz,

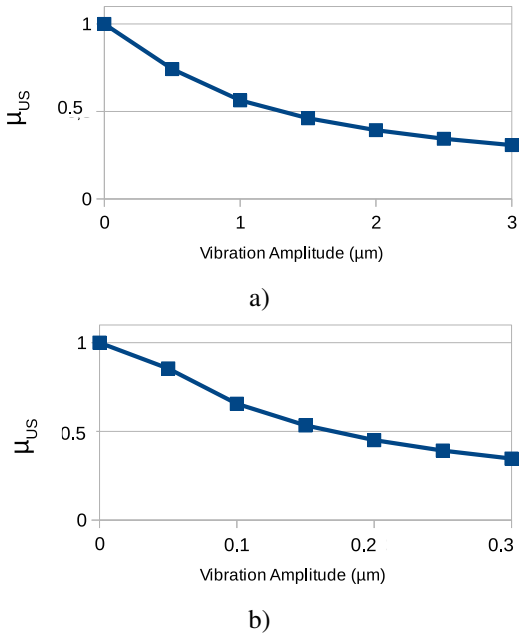

Fig. 6. Friction coefficient as a function of the vibration amplitude (peak-to peak) for a) low b) high frequency.

which is comparable to the friction reduction obtained at 66kHz, but with much lower vibration amplitude. This result is consistent with the conclusion of other works like [9]. The curve depicted in the figure 7 gives the vibration amplitude at high frequency which corresponds to the amplitude at low frequency in order to give the same friction reduction.

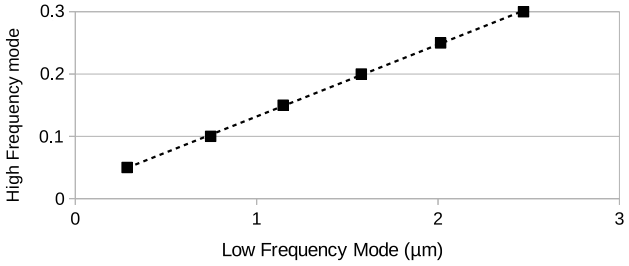

Fig. 7. Vibration amplitude at 200kHz which corresponds to to amplitude at 66kHz for the same friction reduction.

The curve shows a linear behaviour, which slope is equal to 0.12, meaning that a $66kHz$ vibration with an amplitude W produces the same friction as a vibration at 225kHz with an amplitude $0.12 \times W$.

III. DESIGN OF THE HAPTIC SURFACE

A. Device Design

The design of the plate follows the methodology detailed in [12]. Moreover, for the purpose of comparison of the friction reduction at high and low frequency, we want the plate to vibrate around 200kHz and 60kHz. The resulting dimensions of the plate, as well as the implementation of the piezoelectric actuators, are given in the figure 8. We used

two 18mm×5mm×0.3mm piezoelectric actuators with wrap around electrodes for this prototype.

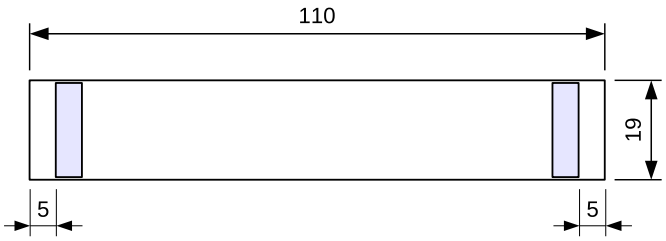

Fig. 8. Design of a 200kHz prototype; plate's thickness is 1.9mm and the material is glass; dimensions are in mm.

An experimental characterization of the plate has been carried out. The resonance modes experimentally identified were equal to 225kHz, with a wavelength of $\lambda = 7.5$mm, and 66kHz with a wavelength of $\lambda = 15$mm.The corresponding cartographies made with a laser interferometer (OFV5110, Polytech, Germany) are given in the figure 9.

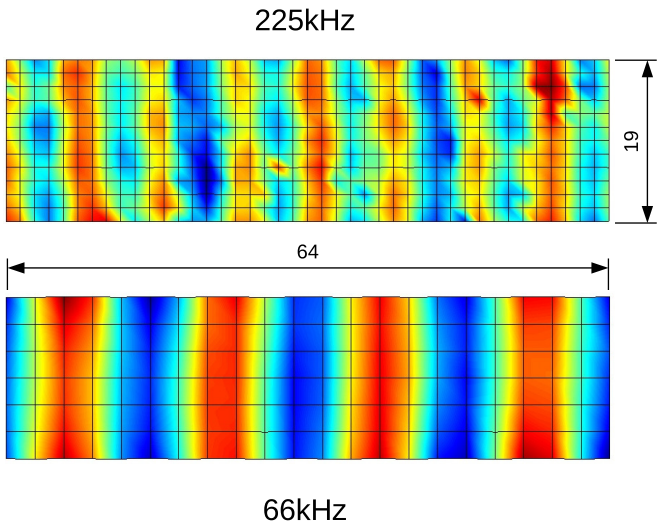

Fig. 9. Measured cartography; dimensions are in mm.

B. Vibration performance

The vibration amplitude at 225kHz is a linear function of the voltage, as depicted figure 10; this shows that the piezoelectric actuators do not saturate, and the power consumption is equal to $P_e = 600$mW at 90nm peak to peak.

The response time of the plate – which is measured when the supply voltage is step varying – is measured and equal to 0.5msec and 1.3msec at 255kHz and 66kHz respectively.

C. Friction Reduction

The plate is put on a 6 axis force/Torque sensor (Nano 43 from ATI/USA). We record the response of the tangential force when the ultrasonic vibration is set on and off for the two vibration modes. The records are depicted in the figure 11. During this test, the vibration amplitude is varying from 0 (the device is switched off) and $194nm$ and 2.8μm peak to peak, for 225kHz and 66kHz respectively. Each step lasts 50ms.

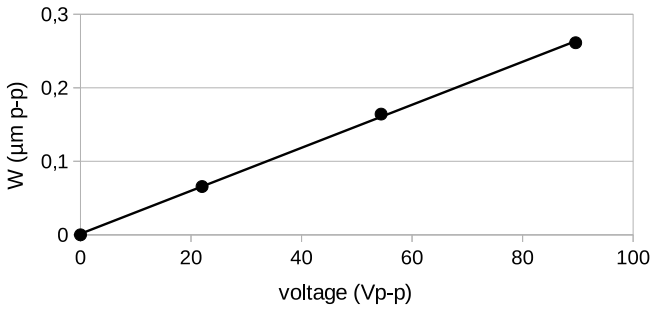

Fig. 10. Plate's deflection as a function of the voltage at resonance; measurement are given in peak to peak values.

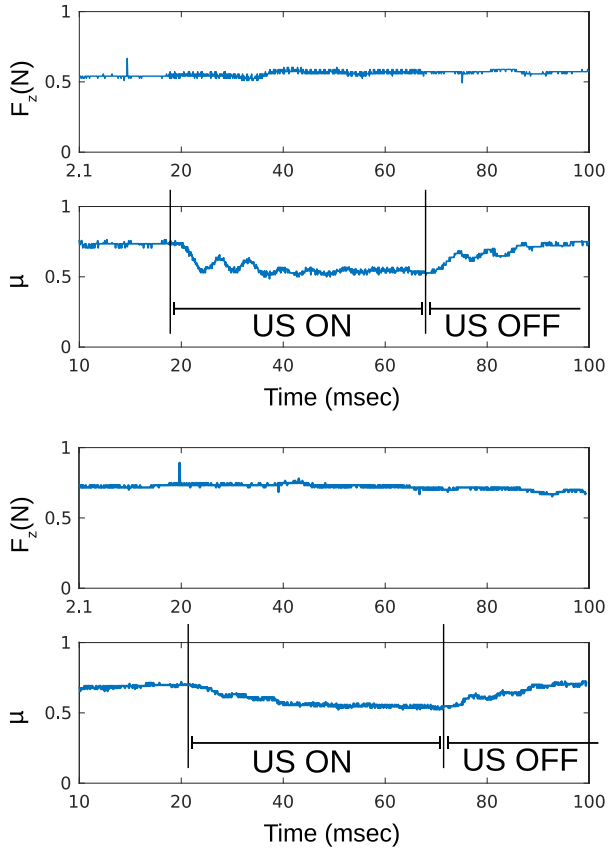

Fig. 11. Friction as a function of time when the ultrasound are switched ON and OFF, and for a user sliding on the plate; top:225kHz, bottom: 66kHz

IV. EXPERIMENTAL EVALUATION

A. Objective and method

The objective of this experimental evaluation is to scale the vibration amplitude on a device working at high frequency with the vibration amplitude at low frequency which gives the same perception (point of Subjective Evaluation). For that purpose, we present to the participants a standard stimulus which consists of a square modulation at 10Hz of the

vibration amplitude on the plate at 66kHz. The participants choose the amplitude at 225kHz which is perceived equally to the standard, following a staircase method with descending trial. We repeat this procedure for each level of vibration amplitude, which are presented randomly to the participants. The participants can switch from the standard to the sample at their convenience.

We have chosen 5 levels (named 1 to 5) for the standard stimulus, each level corresponding to a specific vibration amplitude (0.6μm, 1.2μm, 1.7μm, 2.3μm and 2.9μm respectively). For the comparison samples, which is at high frequency, we have 9 levels (named from 1 to 9) corresponding to 40nm, 70nm, 120nm, 150nm, 200nm, 220nm, 230nm, 240nm, 245nm respectively.

The participants were 8 volunteers from the institution, including some of the authors. After cleaning and drying their hands thoroughly, they were free to slide their index finger on the plate when not powered. Then a low frequency stimulus at level 5 is presented followed by a low frequency stimulus at level 1, which is perceived as less intense. After this training session the participant is instructed about his task by these words: "find the sample which intensity is equivalent to the standard one". Then the test begins, and a sample at a higher or lower level is presented according to the participant's wish.

B. Results

The results for each participant are collected in the figure 12. They present the vibration amplitude at 225kHz which gives the same stimulation amplitude as a standard vibration at 66kHz.

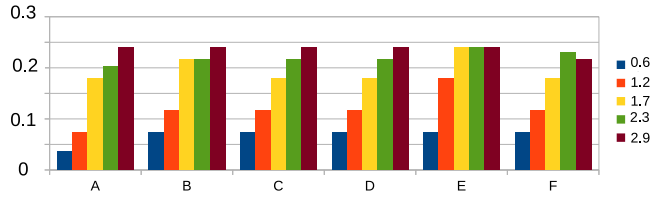

Fig. 12. Participants results sorted according to the vibration amplitude for the low frequency vibration; amplitudes are given in micrometer peak to peak.

In general, the participants have found that increasing the high frequency vibration amplitude gives a higher stimulation intensity, except the participant F, for the highest intensity. Moreover, they could map the vibration amplitude at high frequency to the amplitude at low frequency to obtain a same intensity. The figure 13 depicts the average response as well as the standard deviation for each low frequency intensity.

The averaged response can be approximated to a linear curve, which slope is equal to 0.08, meaning that a 66kHz stimulus with an amplitude W is equal to a 225kHz stimulus with an amplitude $0.08 \times W$.

V. DISCUSSION

The results obtained in this work show that high frequency stimuli require less vibration amplitude. This is demonstrated

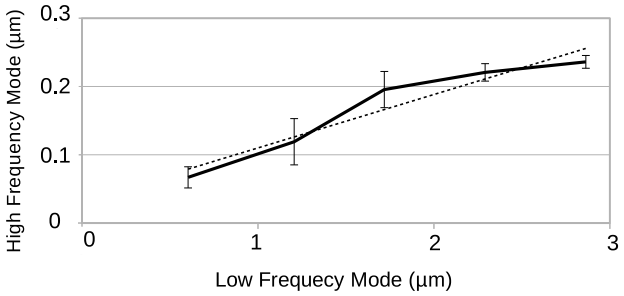

Fig. 13. Plate's deflection as a function of the voltage at resonance; measurement are given in peak to peak values.

by the content of the figures 12 and 13. The figure 11 shows that indeed, a high frequency plate and a low frequency plate produce the same transient response for the friction coefficient. This is consistent with the bed spring model as presented in the first section. Hence, as already found in theoretical analysis, this experimental work demonstrates that frequency plays an important role to reduce the friction with ultrasonic vibration.

The ratio between the high frequency vibration amplitude and the low frequency amplitude corresponding to the same perceived intensity extracted from he psychophysical study (0.08) is lower than the ratio obtained from the modeling in the figure 7 (0.12). It is lower than the ratio of the vibrating speed ($\frac{66}{225} = 0.3$), but in the same order as the ratio of acceleration ($\left(\frac{66}{225}\right)^2 = 0.086$). However, even though the figures are close, we have to take into account two facts that may alter our conclusion. First the two plates do not have the same response time, and the high frequency mode is faster than the slow one, hence increasing the stimulus' intensity. Second, the two modes do not have the same wavelength: the high frequency mode presents one wavelength under the fingertip, while the low frequency mode present only half one, and this could be beneficial to the high one.

In spite of these facts, we can make the hypothesis that, in the process to reduce friction, the acceleration is an invariant, which means that the friction is a function of $(2\pi f)^2 W$ where f is the frequency and W is the vibration amplitude.

VI. CONCLUSIONS

This paper investigates the friction reduction produced by a plate vibrating at high frequency (225kHz), and compares the results with a vibration on the same plate at low frequency (66kHz). The modelling and the psychophysical experiment shows that the vibrating speed is not an invariant for the friction reduction, but it could be the vibration acceleration instead. This trend is confirmed by the analytical modelling based on a bed spring model. However, a more in depth study is necessary in order to analyze the influence of the model parameters on the curve of figure 7, and in particular the values of the damping.

These conclusion are important within the field of Friction reduction based haptic interfaces. Indeed, by increasing the

frequency, much less vibration amplitude is needed. Therefore, the connections to the chassis could be made easier.

AKNOWLEDGEMENT

This work has been carried out within the framework of the IRCICA (Instituts des Composants Logiciels et Matériels pour l'Informatique et la Communication Avancé), and the Mint Project from INRIA. The authors thank Bertrand Leduc for his help in the implementation of the modelling.

REFERENCES

[1] M. Biet, G. Casiez, F. Giraud, and B. Lemaire-Semail, "Discrimination of virtual square gratings by dynamic touch on friction based tactile displays," in *Haptic interfaces for virtual environment and teleoperator systems, 2008. haptics 2008. symposium on*, IEEE, 2008, pp. 41–48.

[2] O. Bau, I. Poupyrev, A. Israr, and C. Harrison, "Teslatouch: Electrovibration for touch surfaces," in *Proceedings of the 23nd annual acm symposium on user interface software and technology*, ser. UIST '10, New York, New York, USA: ACM, 2010, pp. 283–292.

[3] R. H. Osgouei, J. R. Kim, and S. Choi, "Improving 3d shape recognition with electrostatic friction display," *Ieee transactions on haptics*, vol. PP, no. 99, pp. 1–1, 2017.

[4] C. Hudin, J. Lozada, and V. Hayward, "Localized tactile feedback on a transparent surface through time-reversal wave focusing," *Ieee transactions on haptics*, vol. 8, no. 2, pp. 188–198, Apr. 2015.

[5] H. Kim, J. Kang, K.-D. Kim, K.-M. Lim, and J. Ryu, "Method for providing electrovibration with uniform intensity," *Ieee transactions on haptics*, vol. 8, no. 4, pp. 492–496, 2015.

[6] C. D. Shultz, M. A. Peshkin, and J. E. Colgate, "Surface haptics via electroadhesion: Expanding electrovibration with johnsen and rahbek," in *World haptics conference (whc), 2015 ieee*, IEEE, 2015, pp. 57–62.

[7] M. Biet, F. Giraud, and B. Lemaire-Semail, "Squeeze film effect for the design of an ultrasonic tactile plate," *Ieee transactions on ultrasonics, ferroelectrics, and frequency control*, vol. 54, no. 12, pp. 2678–2688, Dec. 2007.

[8] M. Wiertlewski and J. E. Colgate, "Power optimization of ultrasonic friction-modulation tactile interfaces," *Ieee transactions on haptics*, vol. 8, no. 1, pp. 43–53, Jan. 2015.

[9] E. Vezzoli, Z. Vidrih, V. Giamundo, B. Lemaire-Semail, F. Giraud, T. Rodic, D. Peric, and M. Adams, "Friction reduction through ultrasonic vibration part 1: Modelling intermittent contact," *Ieee transactions on haptics*, vol. 10, no. 2, pp. 196–207, Apr. 2017.

[10] T. Nara, M. Takasaki, T. Maeda, T. Higuchi, S. Ando, and S. Tachi, "Surface acoustic wave tactile display," *Ieee computer graphics and applications*, vol. 21, no. 6, pp. 56–63, 2001.

[11] M. Wiertlewski, R. Fenton Friesen, and J. E. Colgate, "Partial squeeze film levitation modulates fingertip friction," *Proceedings of the national academy of sciences*, vol. 113, no. 33, pp. 9210–9215, 2016.

[12] F. Giraud, M. Amberg, B. Lemaire-Semail, and G. casiez, "Design of a transparent tactile stimulator," in *2012 ieee haptics symposium (haptics)*, Mar. 2012, pp. 485–489.